RESEARCH ARTICLE
doi: 10.2306/scienceasia1513-1874.2023.020

ScienceAsia 49 (2023): **275–281**

Protective effects of resveratrol on nerves in rats with Alzheimer's disease

Jun Li[a,b], **Chonghao Yuan**[a,b], **Xiaojun Hu**[a,b,*]

[a] Department of Traditional Chinese Medicine and Acupuncture, Wuhan Puren Hospital, Wuhan University of Science and Technology, Wuhan 430081 China

[b] Department of Rehabilitation Medicine, People's Hospital of Liwan District, Guangzhou 510370 China

[*]Corresponding author, e-mail: canlao599130@163.com

Received 20 Mar 2022, Accepted 8 Aug 2022
Available online 9 Feb 2023

ABSTRACT: Alzheimer's disease (AD), a degenerative disease of the central nervous system, is mainly treated by cholinesterase inhibitors and memantine. We aimed to assess the protective effects of resveratrol (RES) on hippocampal nerves in AD rats. Forty healthy Sprague-Dawley rats were assigned into model, blank, low-dose RES, and high-dose RES groups ($n = 10$). After modeling, RES groups were daily injected with corresponding doses of RES. Their cognitive functions were tested on days 1, 5, 10, and 14. The cellular morphology was compared through hematoxylin-eosin staining. The levels of norepinephrine (NE), dopamine (DA), choline acetyltransferase (ChAT), malondialdehyde (MDA), nitric oxide (NO), reactive oxygen species (ROS), activities of superoxide dismutase (SOD), inducible nitric oxide synthase (iNOS), catalase (CAT), and glutathione peroxidase (GSH-Px) as well as total antioxidant capacity (T-AOC) were detected. The expressions of Kelch-like ECH-associated protein 1 (Keap1) and nuclear factor E2-related factor 2 (Nrf2) were measured using Western blotting. Compared with model group, the escape latency, the balance beam score, the Longa score, and the levels of ROS, MDA, NO, and iNOS activity were significantly decreased in the RES groups ($p < 0.05$); while the platform-crossing times, the levels of NE, DA and ChAT, the activities of CAT, GSH-Px and SOD, T-AOC and protein expressions of Nrf2 and Keap1 were significantly increased ($p < 0.05$). Hippocampal pathological changes were significantly relieved in the RES groups compared with those in the model group. RES exerts protective effects on hippocampal neurons, regulates the neurotransmitter level, and reduces oxidative stress response, probably by activating the Nrf2/ARE pathway.

KEYWORDS: resveratrol, hippocampal nerves, rat model, Alzheimer's disease, neuroprotective mechanism

INTRODUCTION

Alzheimer's disease (AD), a degenerative disease of the central nervous system [1], frequently occurs in elderly patients aged above 65 years old. With population aging, it is estimated that over 130 million people around the world will suffer from AD by 2050 [2]. The pathogenesis of AD has not been completely clarified yet. Many theories have been proposed, such as the amyloid cascade theory [3], cholinergic hypothesis, Tau protein pathogenic theory [4], and oxidative stress response theory [5]. Currently, AD patients are primarily treated with cholinesterase inhibitors [6] and memantine [7], but the therapeutic effects are different. According to the condition of patients, traditional Chinese medicine drugs; characterized by multi-target therapy, mild toxicity, low side effects, and high safety; are additionally applied [8]. Targeted therapy is promising; however, targeted drugs for AD are currently not commercially available, hence further exploration is needed. Resveratrol (RES) is a non-flavonoid polyphenol compound present in a variety of plants, with antitumor, antibacterial, antioxidative, immunoregulatory, cardiovascular and neuronal protective effects [9]. Although RES exerts a neuroprotective effect in AD [10], the mechanism of action remains unclear.

In this study, therefore, AD rat model was established to explore the neuroprotective mechanism of RES for AD patients; and the neuroprotective effects of RES at different doses were compared, aiming to provide novel insights into AD treatment in clinical practice.

MATERIALS AND METHODS

Laboratory animals, reagents and apparatus

Forty healthy Sprague-Dawley rats (about 8 weeks old, 200–230 g, with equal gender ratio) were acquired from the Laboratory Animal Center of Hebei Medical University, China (animal certificate No. SCXK (Hebei) 2019-0003). They were fed freely on water and food and kept at 22–25 °C and 35–40% humidity for 1 week before experiments. The animals were used and processed in accordance with the ethical guidelines for animal experiments.

The following materials were used: RES and D-galactose (purity ⩾ 99%, Sigma, USA); scopolamine (Guangzhou CATO Research Chemicals, China); rat norepinephrine (NE) enzyme-linked immunosorbent assay (ELISA) kits (Cat. No. ml002873), rat dopamine (DA) ELISA kits (ml003201), rat choline acetyltransferase (ChAT) ELISA kits (ml059346) (Shanghai ML-Bio, China); hematoxylin-eosin (HE) (Wuhan Boster Biological Technology, China); reactive oxygen species (ROS) (DCFH-DA fluorescence assay) kit (E004-1-

1), superoxide dismutase (SOD) (hydroxylamine assay) kit (CA001-2-1), glutathione peroxidase (GSH-Px) (colorimetry) kit (A005-1-2), catalase (CAT) (ammonium molybdate assay) kit (A007-1-1), nitric oxide (NO) (nitrate reductase method) kit (A012-1-2), and inducible nitric oxide synthase (iNOS) (H372-1) (Nanjing Jiancheng Bioengineering Institute, China); malondialdehyde (MDA) (TBA method) kit (S0131S) and total antioxidant capacity (T-AOC) (ABTS method) kit (S0121) (Shanghai Beyotime Biotechnology, China); rabbit IgG nuclear factor E2-related factor 2 (Nrf2) primary antibody (12721), rabbit IgG Kelch-like ECH-associated protein 1 (Keap1) primary antibody (8047) and mouse IgG2b β-actin secondary antibody (3700) (Cell Signaling Technology, USA); ECL solution bicinchoninic acid (BCA), protein quantification kit and marker proteins (Thermo Fisher, USA), and polyvinylidene fluoride (PVDF) membrane (Millipore, USA). Other reagents were commercially available and of analytical grade.

The following apparatus were used: Morris water maze and recording analysis system (Shanghai XinRuan Information Technology, China); optical microscope (Leica, Germany); homogenizer (Jiangsu Xundi Instrument Technology, China); microplate reader (Shandong Horde Electronic Technology, China); biochemical analyzer (Shandong BIOBASE Bioindustry, China); Bio-Rad electrophoresis system (Bio-Rad, USA); eBlot™ L1 fast wet transfer system (Nanjing GenScript Biotechnology, China); contact non-destructive quantitative imager (Shanghai e-BLOT Optoelectronics Technology, China); TS-1000 decolorizing shaker and multi-purpose rotating shaker (Jiangsu Haimen Kylin-Bell Lab Instruments, China).

Animal modeling, grouping and intervention

All the 40 rats were randomly divided into 4 groups ($n = 10$): blank, model, low-dose RES (40 mg/kg), and high-dose RES (80 mg/kg) [5]. The model and the two RES groups were subcutaneously injected with 1% D-galactose (5 ml/kg) at the back of the neck daily for 3 weeks to induce subacute senility. Similarly, isometric normal saline was injected to the blank group. From the 4th week, scopolamine (2 mg/kg) was injected into the abdominal cavity for 2 weeks to establish the AD model, while equivalent volume of normal saline was injected at the same site in blank group. After modeling and once per day for 2 weeks, the low-dose and the high-dose RES groups were injected with 40 mg/kg and 80 mg/kg RES, respectively; while isometric normal saline was given to the blank and the model groups.

Detection of spatial learning and memory abilities by Morris water maze

The learning and memory functions of rats were detected by the Morris water maze on day 1, day 5, day 10, and day 14 after drug intervention. In a circular pool (diameter: 1.2 m, height: 0.5 m) filled with (25 ± 1) °C water, 4 points were marked on the wall at a depth of 0.35 m and different positions. A black circular platform (diameter: 10 cm, height: 33 cm) was placed in the center of the pool with the surface 2 cm above the water. During the training and test, the temperature, humidity, light and reference objects outside the water maze remained unchanged, and a quiet environment was maintained. The 4 marked points were used as entry points, from which the rats were put in the pool; and the time of swimming to the platform was recorded. Rats unable to find the platform within 2 min were guided to it by the experimenter. The escape latency was recorded as 120 s. After all the rats stayed on the platform for 30 s, they were re-tested from different entry points. On day 14, the platform was removed, the rats were put into water along the wall, and the number of times crossing the original platform within 1 min was recorded.

Balance beam scoring and Longa scoring

After drug intervention, the behaviors of rats were assessed by balance beam scoring and Longa scoring. The balance beam (70 cm long, 3 cm wide) was placed 10 cm above or parallel to the ground, followed by scoring as follows: 0 point, the rat can jump onto the balance beam, and walk normally without falling; 1 point, the rat can walk on the balance beam, and the probability of falling is $< 50\%$; 2 points, the probability of falling is $\geqslant 50\%$; 3 points, the rat can climb onto the balance beam, and the posterior limb cannot assist in the forward movement; 4 points, the rat can sit on the balance beam but cannot walk; and 5 points, the rat falls off if placed on the balance beam. Longa scorings were as follows: 0 point, no special signs; 1 point, unable to fully stretch the forelimbs; 2 points, limb paralysis and rear-end collision; 3 points, unable to stand or roll; and 4 points, unable to move spontaneously and disturbance of consciousness.

HE staining

After scoring, the rats were decapitated. The hippocampi were harvested on a freezing operating table, and one portion was fixed with 4% formaldehyde solution. Then, the paraffin-embedded hippocampal sections were stained with HE. The sections were deparaffinized twice with xylene (5 min/time), followed by hydration with gradient concentrations of ethanol solutions for 3 min, rinsed with running water, and stained with hematoxylin for 5 min. Afterwards, these sections were rinsed again with tap water, differentiated with 1% HCl-ethanol solution for 30 s, and blued in 0.2% ammonia water for 2 min. Following washing with tap water, they were stained with 0.5% eosin for 10 min and flushed with tap water again, followed by dehydration with gradient concentrations

of ethanol solutions. Finally, they were sealed with neutral balsam, and the images were analyzed under an optical microscope.

Detection of neurotransmitter and related enzyme activity in hippocampi

After flushing with normal saline, the hippocampi were dried with filter papers, weighed and added 9-fold volume of normal saline, followed by processing according to the instructions of ELISA kits, so the sample and standard correctly reacted with solid-phase carriers. Colored substances were produced after enzymatic catalysis, and the optical density was measured with a microplate reader, based on which NE, DA and ChAT were quantified.

Determination of oxidative stress response indices in hippocampi

Some hippocampi were processed according to the kit's instructions. Then the levels of ROS, MDA and NO, as well as iNOS activity, were detected in strict accordance with operating procedures. The activities of GSH-Px, CAT and SOD, and T-AOC were determined using a biochemical analyzer.

Detection of Nrf2 and Keap1 expressions by Western blotting

The nucleoprotein was extracted from some hippocampi with nucleoprotein extraction kits, and quantified by the BCA method, followed by sample preparation and electrophoresis. Following electrophoresis, the protein was transferred onto a PVDF membrane, which was then immersed in Tris-buffered saline with 0.1% Tween20 (TBST) containing 5% skim milk, cultured at room temperature for 1 h, and incubated again with Nrf2 (1:500), Keap1 (1:500) and β-actin antibodies (1:1000) at 4 °C overnight. After equilibration at room temperature for 30 min on the next day, the membrane was flushed with TBST 3 times (5 min/time) and cultured with goat anti-rabbit secondary antibody (1:1000 diluted) for 2 h at room temperature. Afterwards, it was cleaned with TBST 3 times (5 min/time), followed by chemiluminescence assay. Finally, the images were collected, and the gray value was analyzed using ImageJ software.

Statistical analysis

SPSS 16.0 software (IBM, USA) was used for the statistical analysis of data expressed as ($\bar{\chi} \pm s$). The LSD-t test of pairwise comparison was performed. Multigroup comparison was conducted by one-way analysis of variance. $p < 0.05$ suggested a statistically significant difference.

RESULTS

Cognitive function results

The escape latency in the model and the RES groups was significantly longer than the blank group, and in the RES groups was significantly shorter than the model group ($p < 0.05$). There were significantly fewer platform-crossing times in the model and the RES groups than the blank group, and significantly more times in the RES groups than the model group ($p < 0.05$) (Fig. 1).

The balance beam score and Longa score of the RES groups were significantly lower than those of the model group on day 5, day 10, and day 14 ($p < 0.05$).

HE staining results of hippocampi

The results of HE staining showed that the hippocampal neurons were arranged tightly and neatly, and the nuclei were discerned in the blank group. The neurons were arranged disorderly and loosely, and some cells had apoptosis and karyopyknosis in the model group. The neurons were arranged more neatly and tightly, and karyopyknosis was milder in the RES groups compared with the model group (Fig. 2).

Levels of NE, DA, and ChAT in hippocampi

The levels of NE, DA, and ChAT in hippocampi were the highest in the RES groups, followed by the the model group and the blank group ($p < 0.05$) (Fig. 3).

Effects of RES on levels of ROS, MDA, NO, and iNOS activity in hippocampi

The levels of ROS, MDA, NO and iNOS activity in hippocampi of both the low-dose and the high-dose RES groups were significantly lower than that of the model group but higher than the blank group ($p < 0.05$) (Fig. 4).

Effects of RES on levels of SOD, CAT, GSH-Px, and T-AOC in hippocampi

The levels of SOD, CAT, GSH-Px, and T-AOC in hippocampi all significantly declined in the model group compared with the blank group ($p < 0.05$). The levels in the low-dose and the high-dose RES groups were higher than the model group ($p < 0.05$) (Fig. 5).

Effects of RES on protein expressions of Nrf2 and Keap1 in hippocampi

The results of Western blotting revealed that Nrf2 protein expression in hippocampi decreased significantly in the model group in comparison to the blank group ($p < 0.05$). It increased significantly in the low-dose and the high-dose RES groups compared with the model group ($p < 0.05$) (Fig. 6).

The Keap1 expressions in the hippocampi of all the 4 groups were similar. However, the expression of the model group declined compared with the blank and the two RES groups ($p < 0.05$) (Fig. 7).

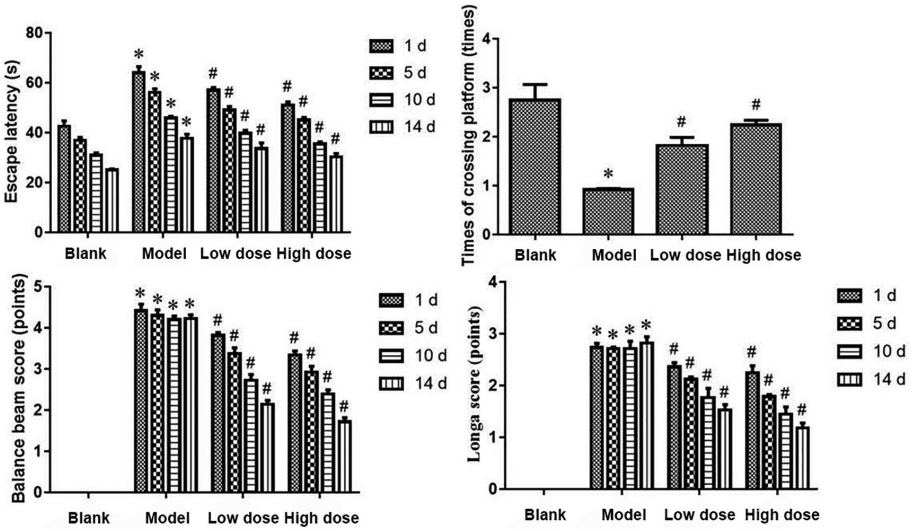

Fig. 1 Cognitive function results. $^{*}p < 0.05$ vs. blank group at the same time point, $^{\#}p < 0.05$ vs. model group at the same time point.

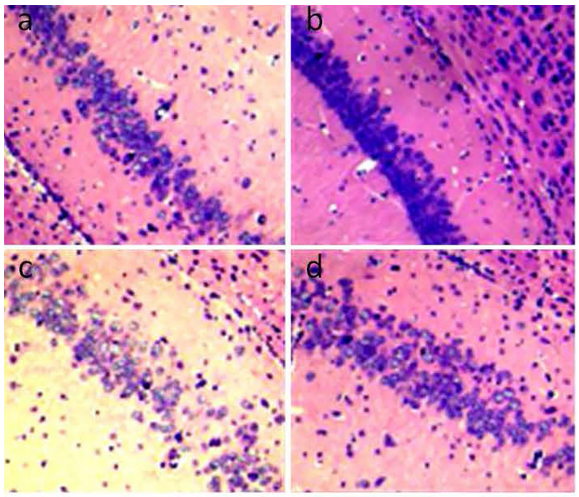

Fig. 2 HE staining results (×400). (a) Blank group; (b) model group; (c) low-dose RES group; (d) high-dose RES group.

DISCUSSION

As a degenerative disease of the nervous system, AD is mainly manifested as progressive cognitive impairment [11]. Its clinical manifestations primarily include memory loss, cognitive disorders, and loss of self-care ability; and one of its pathological manifestations is specific morphological change during hippocampal formation [12]. In this study, the cognitive functions of the low-dose and the high-dose RES groups were superior to the model group, indicating that RES relieved the symptoms of AD. The hippocampus is one of the important structures for the brain memory function, which is related to cognitive impairment [13, 14]. Massive neurons exist in the hippocampus, and hippocampal abnormalities occur due to disordered arrangement of neurons, apoptosis or karyopyknosis, thus, affecting more areas of the brain [15] and ultimately resulting in dementia. Herein, HE staining exhibited that the neurons were arranged loosely, and apoptosis and karyopyknosis occurred in the model group. The neurons were arranged more tightly, and there was less apoptosis and karyopyknosis in the RES groups than the model group. Hence, RES protected hippocampal neurons.

AD affects the neurotransmitter levels in the brain of patients, which, in particular, reduces the content of acetylcholine (Ach) [16]. ChAT and acetylcholinesterase play key roles in keeping the dynamic balance of Ach content, so the activity of ChAT can reflect the level of Ach [17]. NE regulates the cerebral cortex excitability through axons which project to the central nervous system, thereby affecting cognition and emotion. DA has a variety of biological effects, such as alleviation of oxidative stress damage, which synergizes with NE to regulate the excitatory state [18]. In this study, the NE, DA, and ChAT levels in the model group were significantly lower than the blank group. The low-dose and the high-dose RES groups had higher levels of NE, DA, and ChAT than the model group. With the levels in the high-dose RES group higher than the low-dose group, it could be suggested that RES had a regulatory effect on the neurotransmitters in the hippocampi of AD rats.

$A\beta_{1-42}$ can induce the massive accumulation and action of ROS on cell membrane, promoting lipid peroxidation and causing oxidative stress damage. Moreover, it can activate iNOS to produce NO [19]. In

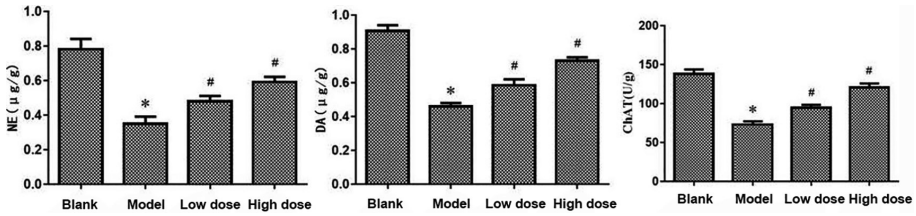

Fig. 3 Levels of NE, DA, and ChAT in hippocampi. * $p < 0.05$ vs. blank group, # $p < 0.05$ vs. model group.

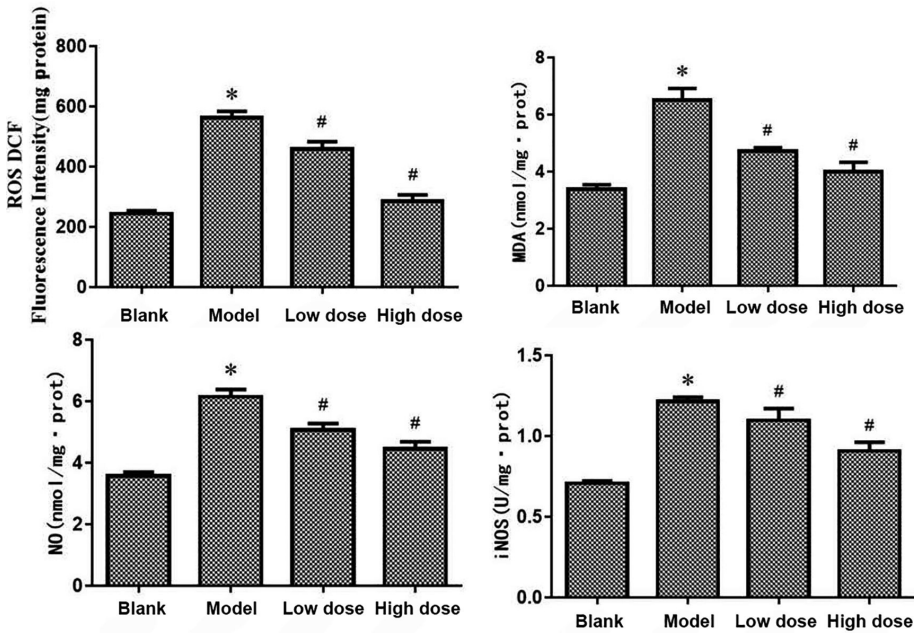

Fig. 4 Levels of ROS, MDA, NO, and iNOS activity in hippocampi. * $p < 0.05$ vs. blank group, # $p < 0.05$ vs. model group.

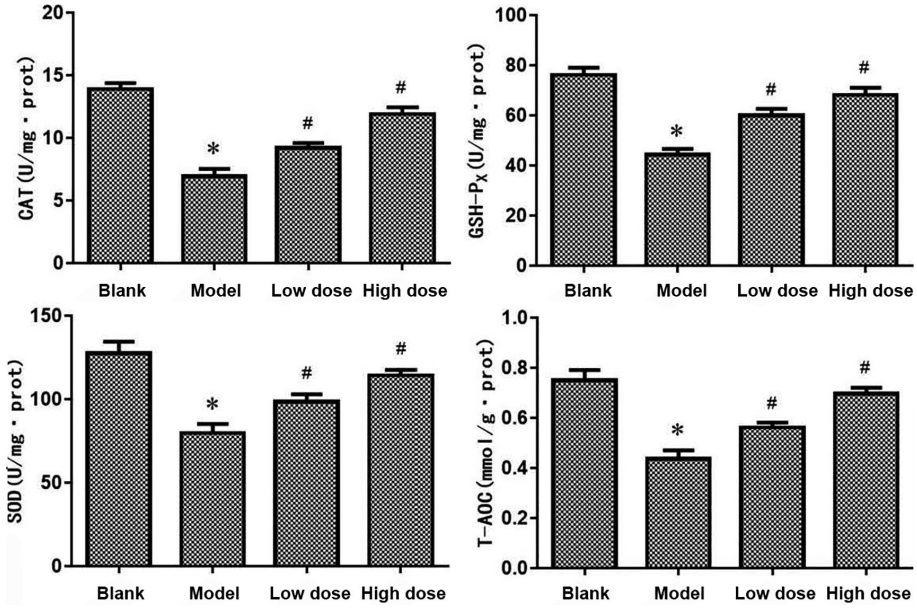

Fig. 5 Levels of SOD, CAT, GSH-Px, and T-AOC in hippocampi. * $p < 0.05$ vs. blank group, # $p < 0.05$ vs. model group.

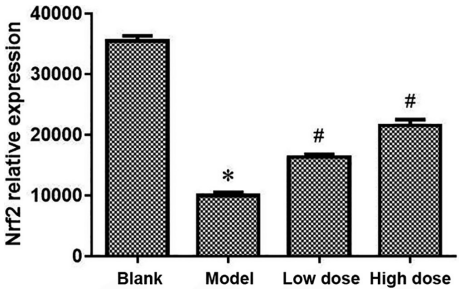

Fig. 6 Protein expression of Nrf2 in hippocampi. $^{*}\,p < 0.05$ vs. blank group, $^{\#}\,p < 0.05$ vs. model group.

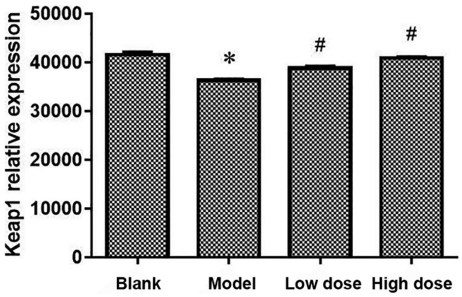

Fig. 7 Protein expression of Keap1 in hippocampi. $^{*}\,p < 0.05$ vs. blank group, $^{\#}\,p < 0.05$ vs. model group.

this study, the levels of ROS, MDA, NO, and iNOS activity in the model group were increased, while the levels of SOD, CAT, GSH-Px, and T-AOC were reduced. The change trends of the above indices in the RES groups were opposite to those in the model group, and the oxidative stress response was suppressed. The results, therefore, indicated that RES alleviated $A\beta_{1-42}$-induced oxidative stress response.

RES can be used for the targeted therapy of AD through regulating a variety of pathways [20]. For example, it motivates the PI3K/Akt/GSK-3β signaling pathway and impedes GSK-3β activity to ameliorate neuronal apoptosis [21]; and it inhibits $A\beta_{1-42}$ deposition and reduces neurotoxicity through regulating the RAGE/LRP1 pathway [22]. Nrf2 is a transcription factor able to regulate antioxidant genes, repair enzymes, and protect cells from oxidative stress, essentially regulating the endogenous antioxidant defense system *in vivo* [23]. Nrf2/antioxidant responsive element (ARE) is a commonly used signal transduction pathway in the studies on changes in oxidative stress response, which can regulate AOC of cells and protect brain tissues [24]. Activated ARE increases the expressions of SOD and CAT, and finally resists oxidative stress damage [25]. In this study, the content of Nrf2 in the model group was significantly lower than the blank group and somewhat lower than the RES groups, with a higher content in high-dose group than the low-dose group. Taken together all these results, RES might enhance the endogenous AOC *in vivo* through activating the Nrf2/ARE pathway, thereby exerting a neuroprotective effect.

CONCLUSION

In conclusion, RES can protect hippocampal neurons, regulate neurotransmitters, and inhibit oxidative stress response in rats with AD, probably by activating the Nrf2/ARE pathway. With obvious therapeutic effects on AD, RES is worthy of wide application in clinical practice. Regardless of the promisingly positive results for treatment of AD patients, ongoing cell and clinical studies are undertaken by our group to validate the findings herein.

REFERENCES

1. Dalvi T, Dewangan B, Das R, Rani J, Shinde SD, Vhora N, Jain A, Sahu B (2020) Old drugs with new tricks: paradigm in drug development pipeline for Alzheimer's disease. *Cent Nerv Syst Agents Med Chem* **20**, 157–176.
2. Brand L, Nichols K, Wang H, Shen L, Huang H (2020) Joint multi-modal longitudinal regression and classification for Alzheimer's disease prediction. *IEEE Trans Med Imaging* **39**, 1845–1855.
3. Gadhave K, Gehi BR, Kumar P, Xue B, Uversky VN, Giri R (2020) The dark side of Alzheimer's disease: unstructured biology of proteins from the amyloid cascade signaling pathway. *Cell Mol Life Sci* **77**, 4163–4208.
4. Majdi A, Sadigh-Eteghad S, Rahigh Aghsan S, Farajdokht F, Vatandoust SM, Namvaran A, Mahmoudi J (2020) Amyloid-β, tau, and the cholinergic system in Alzheimer's disease: seeking direction in a tangle of clues. *Rev Neurosci* **31**, 391–413.
5. Camporez D, Belcavello L, Almeida JFF, Silva-Sena GG, Pimassoni LHS, Morelato RL, do Carmo Pimentel Batitucci M, de Paula F (2021) Positive association of a Sirt1 variant and parameters of oxidative stress on Alzheimer's disease. *Neurol Sci* **42**, 1843–1851.
6. Liou CW, Chen SH, Lin TK, Tsai MH, Chang CC (2021) Oxidative stress biomarkers and mitochondrial DNA copy number associated with APOE4 allele and cholinesterase inhibitor therapy in patients with Alzheimer's disease. *Antioxidants* **10**, 1971.
7. Marotta G, Basagni F, Rosini M, Minarini A (2020) Memantine derivatives as multitarget agents in Alzheimer's disease. *Molecules* **25**, 4005.
8. Pei H, Ma L, Cao Y, Wang F, Li Z, Liu N, Liu M, Wei Y, et al (2020) Traditional Chinese medicine for Alzheimer's disease and other cognitive impairment: a review. *Am J Chin Med* **48**, 487–511.
9. Breuss JM, Atanasov AG, Uhrin P (2019) Resveratrol and its effects on the vascular system. *Int J Mol Sci* **20**, 1523.
10. Rao YL, Ganaraja B, Joy T, Pai MM, Ullal SD, Murlimanju BV (2020) Neuroprotective effects of resveratrol in Alzheimer's disease. *Front Biosci Elite* **12**, 139–149.
11. Zhao J, Yin F, Ji L, Wang C, Shi C, Liu X, Yang H, Wang X, et al (2020) Development of a tau-targeted drug delivery system using a multifunctional nanoscale metal-organic framework for Alzheimer's disease therapy. *ACS Appl Mater Interfaces* **12**, 44447–44458.
12. Uchihara T (2020) Neurofibrillary changes undergoing morphological and biochemical changes – How does

tau with the profile shift of from four repeat to three repeat spread in Alzheimer brain? *Neuropathology* **40**, 450–459.
13. Kuraeiada S, Vattarakorna A, Thamsermsangb O, Akarasereenontb P, Tapechuma S, Tilokskulchaia K, Pakaprota N (2020) The protective effect of Thai Herbal Sahatsatara formula against white matter injury after chronic cerebral hypoperfusion in middle-aged rats. *ScienceAsia* **46**, 713–723.
14. Nie Y, Li S, Yan T, Ma Y, Ni C, Wang H, Zheng H (2020) Propofol attenuates isoflurane-induced neurotoxicity and cognitive impairment in fetal and offspring mice. *Anesth Analg* **13**, 1616–1625.
15. Denoth-Lippuner A, Jessberger S (2021) Formation and integration of new neurons in the adult hippocampus. *Nat Rev Neurosci* **22**, 223–236.
16. Ren JM, Zhang SL, Wang XL, Guan ZZ, Qi XL (2020) Expression levels of the α7 nicotinic acetylcholine receptor in the brains of patients with Alzheimer's disease and their effect on synaptic proteins in SH-SY5Y cells. *Mol Med Rep* **22**, 2063–2075.
17. Jiang S, Xiangxi YI, Shen G (2019) Study on the improvement effects of Lanqian Buccal Tablet on scopolamine-induced learning and memory impairment of mice. *China Pharmacy* **30**, 36–39.
18. Zhou N, Huo F, Yue Y, Yin C (2020) Specific fluorescent probe based on "Protect-Deprotect" to visualize the norepinephrine signaling pathway and drug intervention tracers. *J Am Chem Soc* **42**, 17751–17755.
19. Lei S, Wu S, Wang G, Li B, Liu B, Lei X (2021) Pinoresinol diglucoside attenuates neuroinflammation, apoptosis and oxidative stress in a mice model with Alzheimer's disease. *Neuroreport* **32**, 259–267.
20. Gomes BAQ, Silva JPB, Romeiro CFR, Dos Santos SM, Rodrigues CA, GonÃğalves PR, Sakai JT, Mendes PFS, et al (2018) Neuroprotective mechanisms of resveratrol in Alzheimer's disease: role of SIRT1. *Oxid Med Cell Longev* **2018**, 8152373.
21. Kim EN, Lim JH, Kim MY, Ban TH, Jang IA, Yoon HE, Park CW, Chang YS, et al (2018) Resveratrol, an Nrf2 activator, ameliorates aging-related progressive renal injury. *Aging (Albany NY)* **10**, 83–99.
22. Pannu N, Bhatnagar A (2019) Resveratrol: from enhanced biosynthesis and bioavailability to multitargeting chronic diseases. *Biomed Pharmacother* **109**, 2237–2251.
23. Morris G, Walker AJ, Walder K, Berk M, Marx W, Carvalho AF, Maes M, Puri BK (2021) Increasing Nrf2 activity as a treatment approach in neuropsychiatry. *Mol Neurobiol* **58**, 2158–2182.
24. Yang JE, Jia N, Wang D, He Y, Dong L, Yang AG (2020) Ginsenoside Rb1 regulates neuronal injury and Keap1-Nrf2/ARE signaling pathway in cerebral infarction rats. *J Biol Regul Homeost Agents* **34**, 1091–1095.
25. Huang Z, Ji H, Shi J, Zhu X, Zhi Z (2020) Engeletin attenuates $A\beta_{1-42}$-induced oxidative stress and neuroinflammation by Keap1/Nrf2 pathway. *Inflammation* **43**, 1759–1771.